Periodic pumping tests

Jörg Renner and Mareike Messar

Institute for Geology, Mineralogy, and Geophysics, Ruhr-University Bochum, D-44780 Bochum, Germany. E-mail: renner@geophysik.ruhr-uni-bochum.de

SUMMARY

We performed pumping tests with a periodic succession of injection and production intervals in a field of three shallow boreholes penetrating a jointed sandstone formation. Tests were conducted at periods ranging from 10 to 5400 s and pumping rates between 5 and 20 l min^{-1}. Two types of analysis for the periodic pumping tests are presented. Injectivity analysis rests on the determination of the amplitude ratio and phase shift between the periodic flow rate and pressure records from the pumping well. Interference analysis is based on an evaluation of attenuation and phase shift between the periodic pressure signals at the pumping and monitoring wells. A periodic excitation permits to employ standard signal processing tools, such as fast Fourier transformation, facilitating the evaluation of weak signals. The observed amplitude ratio and phase shift values are compared to analytical predictions of 1-D and radial flow models. Results of interference tests are particularly diagnostic for the applicability of a subsurface model. Our test results do not fully agree with any of the considered analytical models suggesting a heterogeneous subsurface. We suppose that the two analysis methods yield averaged hydraulic properties of different volumes of a heterogeneous subsurface. Periodic injectivity tests screen the subsurface to increasing penetration depth if pumping period is systematically increased, while the subsurface volume between pumping and monitoring well dominates the outcome of an interference test at all periods. Periodic pumping provides several operational advantages compared to conventional testing, such as drawdown, pulse or shut-in tests. Periodic testing can be superposed on a long-term operation reducing operational conflicts and permitting continuous monitoring of changes in subsurface properties. Processing of periodic signals provides results even in a field with strong transient changes in fluid pressure related, for example, to operations in nearby wells. Periodic pumping can be performed in a closed loop minimizing the total fluid volume involved.

Key words: borehole geophysics, fluids in rocks, fractures, hydrology, scale effect, spectral analysis.

1 INTRODUCTION

For many years, hydraulic properties of the subsurface have been successfully constrained based on the analysis of pressure or flow transients following a disturbance of an equilibrium state induced by pumping operations, injection or production (e.g. Fetter 2001; Horne 1992; Matthews & Russell 1967). The results are crucial for exploration of oil or gas and intelligent management of water resources. Evaluation of pumping test records often relies on the assumption that the underground is homogeneous or at least assumes statistical homogeneity beyond a certain length scale (e.g. Dagan 1986; Gelhar 1986). The frequently applied Jacob's method for the analysis of drawdown tests works well even for heterogeneous formations and yields an effective transmissivity (e.g. Meier *et al.* 1998). On the one hand, this finding supports the approach to rely on the simplifying assumption of homogeneity. On the other hand, it indicates that Jacob's method is rather insensitive to heterogeneity and will be of

restricted help if the detection and characterization of heterogeneity are the target of an investigation. Characterization of heterogeneity is crucial for a detailed description of the subsurface flow pattern.

The characterization of subsurface heterogeneity has been addressed in field experiments, theoretical analyses, and numerical approaches. Neuman *et al.* (2004) suggested to characterize subsurface heterogeneity in greater detail by conducting multiple cross-hole interference tests. In numerical modelling approaches, statistical variations are introduced for the hydraulic properties of representative volume elements (REV) comprising the subsurface in which the pumping test is conducted (e.g. Copty & Findikakis 2004; Ye *et al.* 2004). The spatial scale of statistical variations in hydraulic properties is of central importance (Dagan 1986). On the scale of the well distance, Sánchez-Vila *et al.* (1999a) analytically investigated the weighting functions involved in the averaging process inherent to pumping tests in heterogeneous media (see also Oliver 1993). Yet, the respective roles of transport and storage on the outcome

of a pumping test in a heterogeneous medium remain poorly understood. In numerical modelling of drawdown tests the imposed heterogeneity in transmissivity causes an apparent variability in storativity (e.g. Meier *et al.* 1998; Sánchez-Vila *et al.* 1999b). Analysing a large set of observations from field tests, Neuman (1990) suggests to question the REV approach and concludes that flow remains non-Darcian (non-Fickian) on all spatial scales.

Here, we present the background and application of periodic pumping tests. A periodic excitation is firstly beneficial from a practical point of view. Signal processing tools permit separating weak signals of known frequency from a time-series. Relying on signal transmission at prescribed frequencies is common practice in electro-technical applications and constitutes the basis for modern communication technology. From a more fundamental perspective, spectroscopy, that is, the testing at a range of frequencies, is a widely applied, powerful tool to identify different elements of storage (capacitors) and transport (resistors) in complex electrical circuits (e.g. Macdonald 1987). Owing to the formal similarity between electrical and hydraulic transport (e.g. Bredehoeft *et al.* 1966; Isakoff 1955) similar diagnostic potential of pumping tests at various frequencies may be expected for hydraulic networks. In fact, during preparation of the manuscript we became aware that based on numerical modelling, Copty & Findikakis (2004) suggested that 'a pumping scheme consisting of several on/off cycles extends the time duration where the response of the heterogeneous system differs from that of an equivalent homogenous system and, hence, can potentially improve the estimate of the variance from the drawdown data'.

In our presentation, we follow the common terminology that an analysis of the pressure response in a monitoring well to a pumping operation in a second well is addressed as an *interference* test (e.g. Matthews & Russell 1967). If flow rate and pressure at the pumping well are measured, we speak of *QP-analysis* and use the term *injectivity* in a collective sense for the relation between flow rate and pressure, that is, covering both, *yield* during drawdown/production (e.g. Schad & Teutsch 1994) and *injectivity index* during pressurization/injection (e.g. Matthews & Russell 1967). Similarly, injection pressure denotes the pressure in the pumping (injection) well irrespective of the sign of flow.

Our approach extends pulse testing (e.g. Johnson *et al.* 1966; Kamal & Brigham 1975; Stegemeier 1982). Pulse testing and drawdown tests do not significantly differ in procedure other than duration but evaluation is based on different parts of the pressure records. Furthermore, our approach is related to harmonic transfer function determination (Crosnier *et al.* 1985) and the sinusoidal oscillation method (e.g. Fischer 1992; Kranz *et al.* 1990; Stewart *et al.* 1961), both previously performed in the laboratory, but differs from the analysis of damped free oscillations of a borehole-aquifer system in response to sudden changes in boundary conditions (Krauss-Kalweit 1987). Previously, only theoretical studies investigated the potential of harmonic testing for oil-well characterization (Hollaender *et al.* 2002; Kuo 1972). The objectives of our work are to test the feasibility of periodic pumping tests and to explore the sensitivity of results to subsurface heterogeneity. Since the periodic tests are performed in a field of three boreholes penetrating jointed sediments they may provide constraints on the constitutive modelling of fractured media. When addressing flow in jointed formations or fissured aquifers it has been common practice to change the model with the increase in considered spatial scale from flow on an individual joint to flow through a finite number of joints with statistically distributed properties to flow through a quasi-continuous medium with averaged hydraulic properties (e.g. Bear 1993; Bear & Berkowitz 1987). To provide a framework for the discussion of observations we estimate equivalent hydraulic parameters relying on steady state solutions of the diffusion equation for boundary conditions at the wall of the pumping borehole that are periodic in time.

2 EXPERIMENTAL DETAILS AND BACKGROUND

2.1 Boreholes

The three boreholes with depths between 20 and 30 m and diameters between 80 and 110 mm are located at the southern city-limits of Bochum, Germany. They form a triangle with side lengths of 20.60, 38.15, and 64.00 m between the northwestern banks of an artificial fresh water reservoir (Kemnader See), and the almost vertical, approximately 15 m high wall of a vacated sandstone quarry (pit Küper & Käseberg; Fig. 1a). The base of the quarry was filled with an up to 4-m-thick layer of a conglomerate of soil, clay, and pebbles to level the terrain (Fig. 1b). Two of the three boreholes are vertical (BK1 30.0 m deep and BK3 20.0 m deep); one (BKs, true vertical depth 27.8 m) dips with ~60° almost pointing south and vertically penetrating the sedimentary bedding. Outcrop measurements reveal that the sandstone is dissected by four joint systems of which one is parallel to the bedding. Borehole logging shows that joints with a spacing of tens of centimetres do exist to the drilled depths. A major, steep fault crops out between BK1 and BK3 approximately perpendicular to the tie line between the two wells. The boreholes are finished with 2-m-long casings at the top (Fig. 1c).

The penetrated lithology is dominated by thick layers of mostly coarse-grained sandstones of the upper carboniferous (Westfal A) but zones of siltstone are also encountered accounting for less than a fifth of the drilled cores. The sandstone and siltstone exhibit average densities of 2.49 and 2.66 g cm^{-3} and corresponding low porosities of about 7 and 5 per cent, respectively.

2.2 Pumping procedure and equipment

We performed periodic pumping tests with periods between 10 and 5400 s. Individual tests comprised 4–30 full periods. A single period consisted of the succession of (1) injection, (2) no-pumping, (3) production and (4) no-pumping operations with relative durations of the pumping and no-pumping sequences of $t_{\text{injection}}/t_{\text{no-pumping}} = t_{\text{production}}/t_{\text{no-pumping}} = 8/7$ (Fig. 2a). Note, we adopt the sign convention that injection and production correspond to positive and negative flow rates, respectively. The pumping protocol yield a periodic pressure signal in the injection well resembling a sinusoidal variation (Figs 2a and b). Two test series deviated from the described protocol. During one experiment, the water level was kept below the natural level by continuous production; the periodic signal was generated by modifying the production rate systematically. For tests with a period of 10 s, injection and production sequences of 5 s length immediately followed each other. In order to compare the results of the periodic tests with conventional tests, drawdown tests were also conducted. Hollow cylinders of diameters between 90 and 110 mm and pneumatic bladders (Ulisch GmbH) were lowered in the monitoring boreholes to systematically vary their storage capacity (Fig. 1c).

Pressure loggers (Hope Hydrology) with a resolution of 0.1 mbar and an accuracy of better than 5 mbar were placed between 1 and 2 m below the natural water level of the three boreholes. The sampling interval was kept at 1 s. Water level changes in the boreholes
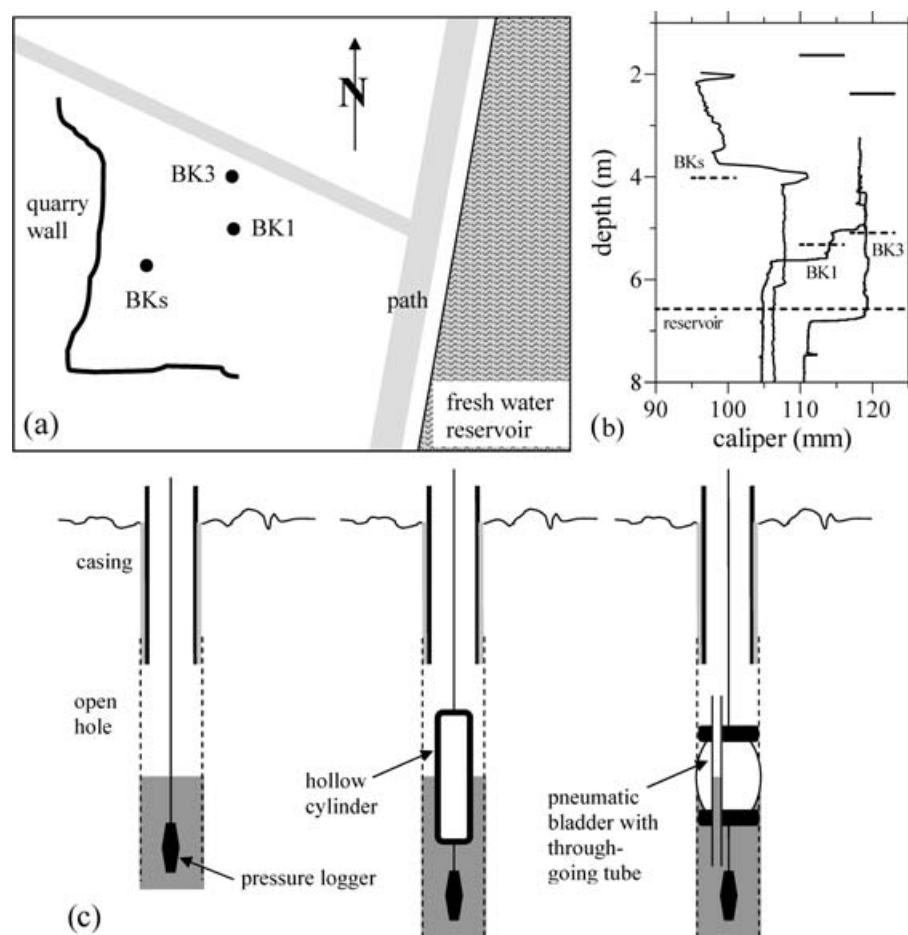
Figure 1. (a) Sketch of the borehole site. (b) Calliper of the three boreholes with depth given with respect to BKs. Surface levels with respect to BKs are indicated by the solid horizontal lines. The steps in the callipers of BK1 and BK3 indicate the transition from the land filling to the sedimentary rock basement. The average natural groundwater levels (dotted horizontal lines) systematically fall toward the reservoir. (c) Set-up of injection and monitoring wells. Water level variations were recorded with pressure loggers. Hollow cylinders and pneumatic bladders were used to vary the storage capacity of monitoring wells.
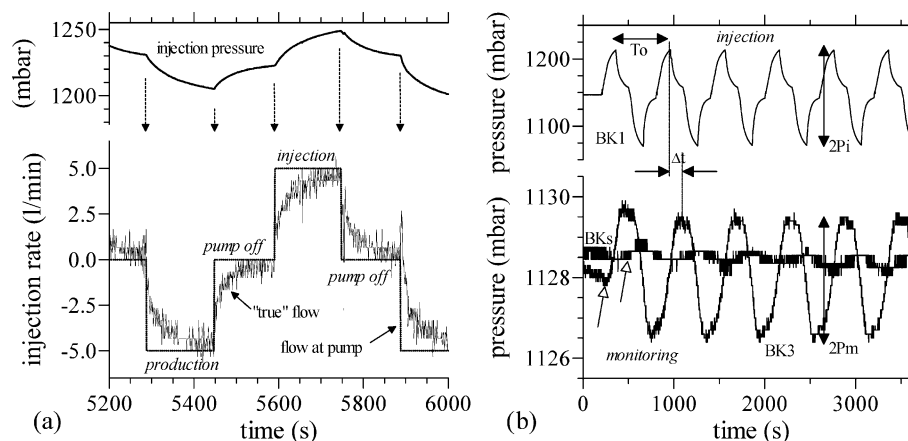

Figure 2. (a) Example for the construction of an injection rate record. The arrows indicate how onset and termination of pumping were deduced from vertices in the injection pressure record. The flow recorded at the pump was then corrected for the storage effect according to eq. (1) to gain the true flow into the formation. (b) Example of pressure observations in response to a periodic pumping test in borehole BK1 with a period $T_0 = 10$ min. Note the significant difference in scales of the two pressure axes. For the record in monitoring well BK3, arrows graphically illustrate the determination of attenuation, the ratio between pressure amplitude in the monitoring and the injection well, $\delta_{pp} = p_m/p_i$, and phase shift, the normalized delay between monitoring and injection pressure, $\varphi_{pp} = \Delta t/T_0$. The arrows with white heads mark the onset of the response, which occurs during the first cycle of pumping.

were induced using a jet pump (maximum flow rate $\sim$23 l min^{-1}) and a manifold for switching between production and injection. Flow between a storage barrel and the injection well was monitored directly at the pump. Subsurface injection rates were determined by constructing a synchronized flow record using the pronounced vertices in the pressure records at the start and end of pumping operations (see Fig. 2a). The fluid storage associated with rise and fall of the water level in the injection well was corrected relying on borehole radii r_i from a calliper log (Fig. 1b). The flow injected into (produced from) the formation, Q_i, was calculated from the flow at the pump, Q_{pump}, as

$$Q_i = Q_{\text{pump}} - \frac{A_i}{\rho g} \dot{p}_i, \tag{1}$$

where $A_i = \pi r_i^2$ and $\dot{p}_i$ denote the cross-section of the injection well and the time derivative of the injection pressure, respectively.

2.3 Processing of pressure and flow records

Characteristics of pressure and flow records were determined using fast Fourier transformation (FFT) analysis. Fourier analysis reveals periodicities in time-series and the relative strengths and phases of periodic components; a digitally recorded signal is reduced to amplitude and phase of oscillations at distinct frequencies whose values are determined by the sampling rate and the record length (amplitude and phase spectra) (e.g. Buttkus 2000). Our records constitute finite time-series comprising at least four and up to 30 full oscillations. For the analysis, we cut the record length to multiples of the imposed pumping period. Data were not detrended, that is, first and last value in an analysis window could differ. Simultaneous transformation of a pair of records (either injection and monitoring pressure or injection pressure and rate) permits determining the dimensionless delay, the phase shift, and the amplitude ratio between the spectral components of these signals (Fig. 3). If injection and monitoring pressure are compared, the amplitude ratio is dimensionless, too, and is referred to as attenuation.

The resolution in phase shift is far better than the time step of data acquisition. In theory, the determined phase shift values are exact since the Nyquist frequency is small compared to even the fastest tests. Noise at a frequency slightly higher than the Nyquist frequency could potentially cause aliasing but no such source is obvious. In fact, spectra decay strongly toward high frequencies (Fig. 3a). FFT analysis can determine the phase shift between two signals within one cycle. To obtain the absolute delay between two signals the actual onset of the response has to be identified. Here, we refrained from more sophisticated methods such as correlation analysis and determined the onset by eye whenever this approach was unambiguous (see Fig. 2b). For the majority of tests, the onset of pressure oscillation occurred in the monitoring wells within the first cycle (Table 1). The early response is biased by a transient since in contrast to the assumption for the theoretical solutions a causal periodic function is employed.

Variability and temporal evolution of phase shift and amplitude ratios were investigated by a sliding window analysis. The window, for which the FFT analysis was performed, had a length of two or more periods of the pumping operation and was successively shifted along the record by steps of a tenth to a third of a period. Amplitude ratio and phase shift values are only reported if indeed a local maximum in the amplitude spectrum occurs at the pumping frequency; the variability gained from the sliding window analysis is used as a measure of the uncertainty.

2.4 Inversion of observations toward hydraulic properties

A continuum description of fluid flow in porous media leads to Navier–Stokes equations (e.g. Hilfer 1996). Viscous skin depth $\delta = \sqrt{\mu T_0/(\pi\rho)}$ is the scaling parameter indicative for the transition from fluid viscosity- to inertia-controlled fluid transport (e.g. Bernabe 1997; Olny & Boutin 2003) where μ and ρ denote the viscosity and density of the fluid, respectively. If the viscous skin depth falls below the characteristic width of the conduits then inertia effects become significant. The estimated range of $\delta \simeq 2, \ldots, 40$ mm for our periodic tests with periods of $T_0 = 10, \ldots, 5400$ s and $\mu \simeq 1 \cdot 10^{-3}$ Pa $\cdot$ s and $\rho \simeq 1000$ kg m^{-3} for water clearly exceeds characteristic pores sizes and also the likely opening of the joints and, therefore, inertia effects can be excluded. The fluid viscosity-controlled part of Navier–Stokes equation assumes the form of a diffusion equation when Darcy's law and a linear mechanical constitutive equation for the porous medium constraining compressibility are applicable. Hydraulic diffusivity constitutes the characteristic material parameter of the diffusion equation quantifying the ratio between transport and storage properties, $D = \frac{T}{S} = \frac{k}{\mu\beta_s}$, equally presented by a pair of borehole-related hydraulic parameters

(1) transmissivity T [m^{2}s^{-1}] and storativity S [-], or a pair of material characteristics

(2) permeability

$$k = \frac{\mu}{\rho g h} T \simeq \frac{10^{-7}\,\text{m} \cdot \text{s}}{h} T \,[\text{m}^2]$$

and specific storage capacity $\beta_s = \frac{S}{\rho g h} \simeq \frac{10^{-4}\,\text{m} \cdot \text{Pa}^{-1}}{h} S$ [Pa^{-1}]. Here, $g \simeq 10$ m s^{-2} and h denote the gravitational acceleration and the height of the injection zone, respectively.

Classic evaluation of hydraulic tests is based on analytic solutions of the diffusion equation for radial flow in a homogeneous medium. The resulting estimates of hydraulic parameters constitute properties of an equivalent homogeneous medium in the sense that the responses of the real medium and the hypothetical homogeneous medium to the pumping operation are 'indistinguishable' (e.g. Barker & Black 1983; Renard & de Marsily 1997; Sánchez-Vila *et al.* 1999b). In order to determine such equivalent hydraulic parameters, we investigated the solution of the diffusion equation for radial flow in a homogeneous medium for periodic boundary conditions at the pumping well (Appendix).

Sinusoidal pressure variations with a period $T_0 = 2\pi/\omega$ in an infinitely long pumping well with radius r_i are transmitted into a homogeneous isotropic medium over a distance r with attenuation

$$\delta_{pp} = \left| \frac{K_{0(\eta r)}}{K_{0(\eta r_i)}} \right|, \tag{2}$$

and phase shift

$$\varphi_{pp} = \arg\left(\frac{K_{0(\eta r)}}{K_{0(\eta r_i)}} \right). \tag{3}$$

The complex parameter $\eta \equiv \sqrt{i\omega/D}$ has the unit [m^{-1}] and carries the hydraulic properties and test characteristics. Bessel functions, K_0, of the second kind and zero order determine the solution for the assumed radial symmetry (Abramowitz & Stegun 1965). When pumping pressure is increased and decreased, fluid is lost into and gained from the formation, respectively. Therefore, flow rate and pressure also exhibit a characteristic phase shift and amplitude ratio.
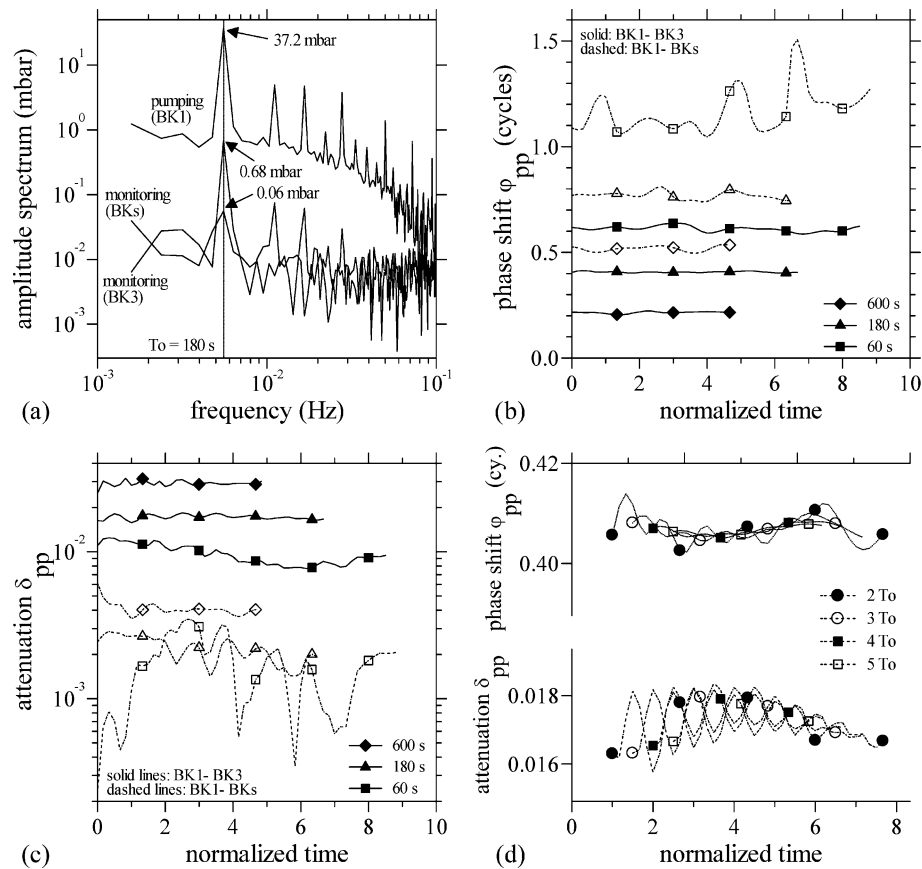
Figure 3. (a) Examples of amplitude spectra of pressure records in the pumping and the two monitoring wells of a periodic pumping test in BK1 with a period of 180 s (frequency of $5.5 \cdot 10^{-3}$ Hz). The amplitudes at the pumping frequency are indicated (compare Table 1) and correspond to the global maximum in each spectrum; local maxima occur systematically at higher frequencies corresponding to the deviation of the pumping signal from a true sinusoidal oscillation. Temporal evolution of (b) phase shift and (c) attenuation of pressure records of pumping tests with periods of 60, 180 and 600 s gained from a sliding window analysis with a window length of two periods and a step length of one-sixths of a period. Time is expressed as multiples of the imposed period. (d) Results of the FFT-analysis of a periodic pumping test with a period of 180 s using sliding windows with a length of two to five periods.

Flow rate is actually ahead of the pressure by a phase shift

$$\varphi_{qp} = \arg\left(\frac{\eta K_{1(\eta r_i)}}{K_{0(\eta r_i)}}\right), \tag{4}$$

and the amplitude ratio amounts to

$$\delta_{qp} = \frac{2\pi r_i T}{\rho g}\left|\frac{\eta K_{1(\eta r_i)}}{K_{0(\eta r_i)}}\right|, \tag{5}$$

where Bessel functions, K_1, of the second kind and first order describe the flow rate (Appendix). In contrast to the relation between injection and monitoring pressure, the complex injectivity explicitly depends on hydraulic diffusivity and transmissivity yielding separate constraints on the transport and the storage contribution to hydraulic diffusivity. The occurrence of Bessel functions prevents an analytical inversion toward hydraulic parameters. One has to rely on numerical forward calculation graphically illustrated in the Appendix.

2.5 Relation between temporal and spatial scales of flow processes

Diffusion processes obey a simple scaling relation between the diffusion coefficient, D, the characteristic distance, l_c, and the characteristic time, t_c, of a transport process, $D \sim l_c^2/t_c$ (e.g. Turcotte & Schubert 1982). If Darcy's law is valid and the physical properties of the fluid and the solid medium are constant, fluid flow constitutes a

diffusion process, and the above scaling applies to the experimental duration and spatial extent of pressurization. Specifically, the characteristic penetration depth, r_p, of a pressure pulse imposed during a periodic pumping test with period T_0 can be estimated as

$$r_p \sim \sqrt{DT_0}. \tag{6}$$

This scaling concept has been qualitatively applied to heterogeneous aquifers, too (e.g. Schad & Teutsch 1994). Numerical work indicates that heterogeneity in transmissivity and storativity differently affect the geometry of influence zones of well tests (Oliver 1993). Furthermore, strong heterogeneity may lead to a breakdown of the Darcy relation (Neuman 1990). Nevertheless, it seems a reasonable approach that the correlation between penetration depth and elapsed time will remain positive at least on average as long as the relation between pressure pulse and response is causal. Therefore, we will rely on eq. (6) for zero order estimates of the spatial scale involved in a test at an applied pumping period.

3 RESULTS

3.1 Periodic pumping tests

We performed a total of about 40 tests with periodic excitation (Table 1). The deviation of pressure signals from a true sinusoidal

Table 1. Conditions and results of the performed periodic pumping tests. Hydraulic properties (diffusivity, transmissivity, and storativity) are determined assuming radial flow in an isotropic homogeneous subsurface (eqs 2–5; Appendix). The set-up of the monitoring wells is given as the diameter of the inserted cylinder (0: open well; bla.: bladder; see Fig. 1). (nd: not determined; ∗: onset of periodic response unclear; a: after extended production; b: superposed by continuous production).

The columns are grouped as: **Pumping (injectivity)** (pumping well — upper block **BK1**, lower block **BK3**) and **Monitoring (interference)** — first monitoring set (**BK3** for BK1-pumping block, **BK1** for BK3-pumping block) and second monitoring set (**BKs**).

Period T_0 (s)	Amplit. p_i (mbar)	Amplit. ratio δ_{qp} (1 min^{-1}/mbar)	Phase shift φ_{qp} (cycles)	Hyd. diff. D_{qp} (m^2 s^{-1})	Transmiss. T (m^2 s^{-1})	Storativity S (−)	Attenu. δ_{pp} (−)	Hyd. diff. D_δ (m^2 s^{-1})	Phase shift $-\varphi_{pp}$ (cycles)	Hyd. diff. D_φ (m^2 s^{-1})	Set-up/ diam. (mm)	Attenu. δ_{pp} (−)	Hyd. diff. D_δ (m^2 s^{-1})	Phase shift $-\varphi_{pp}$ (cycles)	Hyd. diff. D_φ (m^2 s^{-1})	Set-up/ diam. (mm)
		BK1 (pump)					*BK3 (monitor)*					*BKs (monitor)*				
5400	18.2	0.2656	0.0152	2.84E+1	5.56E−4	1.96E−5	0.0627	0.25	0.0821	2.49	100	0.0032	0.07	0.2540	0.48	90
1800	35.6	0.2615	0.0459	1.03E−3	1.84E−4	1.78E−1	0.0417	0.44	0.1409	1.67	0	0.0062	0.32	0.2395	1.59	0
1800	34.1	0.3037	0.0270	7.11E−2	3.77E−4	5.30E−3	0.0476	0.51	0.1220	2.38	100	0.0040	0.24	0.2758	1.15	90
1800	14.0	0.3157	0.0232	2.89E−1	4.49E−4	1.60E−3	0.0450	0.48	0.1193	2.52	100	0.0070	0.34	0.2980	0.98	90
1800	41.2	nd	nd	nd	nd	nd	0.0428	0.45	0.1154	2.69	bla.	0.0049	0.28	0.3085	0.91	bla.
600	55.0	0.3404	0.0613	4.78E−4	1.61E−4	3.37E−1	0.0280	0.83	0.2601	1.14	0	0.0030	0.63	0.5224	0.84	0
600	29.2	0.2856	0.0859	4.57E−5	6.80E−5	1.49	0.0247	0.73	0.2434	1.29	0	0.0010	0.38	0.4845	1.01	0
600	55.8	0.3386	0.0468	2.75E−3	2.31E−4	8.40E−2	0.0290	0.86	0.2169	1.73	100	0.0038	0.70	0.4700	1.09	90
600	25.6	0.3473	0.0426	5.22E−3	2.65E−4	5.08E−2	0.0301	0.90	0.2178	1.72	100	0.0032	0.65	0.4192	1.37	90
600	12.1	0.3469	0.0380	1.23E−2	3.03E−4	2.46E−2	0.0273	0.81	0.2190	1.65	100	0.0043	0.76	0.4179	1.37	90
600	54.9	0.3307	0.0476	2.42E−3	2.21E−4	9.00E−2	0.0296	0.87	0.2172	1.73	100	0.0040	0.72	0.5171	0.87	90
600	34.4	nd	nd	nd	nd	nd	0.0282	0.83	0.2030	2.01	bla.	0.0054	0.87	0.4533	1.19	bla.
180	24.4	0.6586	0.1459	2.94E−4	1.25E−4	4.26E−1	0.0127	1.38	0.4637	1.05	0	0.0008	1.13	0.7716	1.24	0
180	37.2	0.4237	0.0791	2.28E−4	1.55E−4	6.80E−1	0.0184	1.81	0.3863	1.55	110	0.0015	1.51	0.6232	1.91	0
180	14.0	0.5694	0.0816	1.07E−4	7.93E−5	7.42E−1	0.0169	1.73	0.3814	1.59	110	0.0003	0.80	0.9040	0.87	0
180	9.3	0.3779	0.0897	4.20E−5	1.07E−4	2.55	0.0173	1.74	0.3808	1.59	110	0.0005	0.99	0.7600	1.27	0
180a	7.4	0.7284	0.0987	2.94E−4	1.21E−4	4.10E−1	0.0133	1.43	0.4763	1.03	0	0.0039	2.42	0.5854	2.20	0
180	37.4	0.4100	0.0789	1.70E−4	1.32E−4	7.80E−1	0.0177	1.78	0.4066	1.38	100	0.0022	1.78	0.7694	1.24	90
180	30.4	0.5340	0.0849	nd	nd	nd	0.0115	1.26	0.4552	1.10	0	0.0009	1.20	0.6949	1.52	0
180b	30	nd	nd	nd	nd	nd	0.0178	1.82	0.3702	1.68	bla.	0.0039	2.42	0.6115	2.00	bla.
60	19.0	0.5909	0.1051	5.78E−5	6.29E−5	1.09	0.0067	2.50	0.6785	1.38	0	0.0016	4.65	1.1246	1.44	90
60	18.3	0.6384	0.0984	1.29E−4	9.48E−5	7.30E−1	0.0097	3.38	0.6135	1.70	100	0.0023	5.50	∗.6889		bla.
60	17.9	nd	nd	nd	nd	nd	0.0132	4.30	0.5431	2.20	bla.					
30	10.8	0.8523	0.0715	3.54E−3	3.11E−4	9.00E−2	0.0042	3.97	0.7030	2.51	0					
30	11.2	0.7686	0.0919	5.10E−4	1.49E−4	2.90E−1	0.0060	5.00	0.7209	2.39	100					
30	11.2	nd	nd	nd	nd	nd	0.0105	7.23	0.6024	3.62	bla.					
10	4.1	3.2487	0.1401	nd	nd	nd										
		BK3 (pump)					*BK1 (monitor)*					*BKs (monitor)*				
1800	113.8	0.1739	0.0258	1.01E−1	2.24E−4	2.20E−3	0.0350	0.35	0.1147	2.88	100	0.0017	0.46	0.4424	1.20	90
1800	73.3	nd	nd	nd	nd	nd	0.0380	0.40	0.1069	3.50	bla.	0.0019	0.48	0.4568	1.05	bla.
600	21.2	0.1919	0.0512	1.57E−3	1.18E−4	7.50E−2	0.0227	0.68	0.2200	1.64	100	0.0006	0.87	0.5075	2.50	90
600	85.0	0.2113	0.0371	1.39E−2	1.88E−4	1.35E−2	0.0173	0.52	0.2656	1.09	0	0.0009	1.05	0.6342	1.56	0
600	58.4	nd	nd	nd	nd	nd	0.0246	0.73	0.2025	2.02	bla.	0.0016	1.31	0.5351	2.26	bla.
180	52.2	0.2353	0.0530	4.07E−3	1.37E−4	3.38E−2	0.0069	0.91	0.4575	1.08	0	0.0004	2.64	∗.7844		0
180	34.5	nd	nd	nd	nd	nd	0.0154	1.59	0.3923	1.51	bla.	0.0007	3.17	∗.7323		bla.
60	23.9	0.3634	0.0400	7.86E−2	2.96E−4	3.8E−3	0.0058	2.47	0.6153	1.70	100					
30	12.9	0.6295	0.0338	5.32E−1	6.12E−4	1.1E−3	0.0035	3.62	0.7507	2.18	100					
10	5.1	1.6177	0.1865	nd	nd	nd										

input leads to systematic local maxima in the amplitude spectrum in addition to the global maximum at the main frequency of the pumping procedure (Fig. 3a). The present evaluation restricts to the main frequency. The sliding window analysis reveals that systematic temporal evolutions in amplitude or phase of signals do not occur (Figs 3b and c) indicating that a steady state is reached within about one period. Variability of the determined signal characteristics increases significantly with decreasing period and increasing distance between wells. Increasing the length of the sliding window dampens the excursions (Fig. 3d) that are partly systematic since we did not detrend data.

Interference (PP-)analysis

The observed attenuation and phase shift values between the pressure signals in the pumping and monitoring wells range from 0.0004 to 0.1 and from 0.1 to 2 cycles, respectively (Fig. 4a, Table 1). The reproducibility is high, in particular, for the experiments between the closest wells, BK1 and BK3, where significant pressure response occurs. Generally, the smaller the oscillation period, the less the amplitude and the larger the delay of the monitoring pressure signal. Observed pairs of attenuation and phase shift deviate significantly from the analytical predictions of the considered models, radial and 1-D flow with and without constant-pressure or no-flow boundaries Fig. 4a). Data seem to group in amplitude ratio according to distance. While the ranges in phase shift overlap for the three combinations of wells representing distances between 20 and above 60 m, attenuation values are systematically lower the larger the distance. Each pair of attenuation and phase shift values yields two estimates of equivalent hydraulic diffusivity for the radial flow model (see Appendix). Throughout this paper we exclusively report equivalent hydraulic properties estimated assuming radial flow in a homogeneous medium and, therefore, drop the attribute 'equivalent' from here on. On average, hydraulic diffusivity amounts to ~ 2 m^{2}s^{-1} (Fig. 4b), but we find differences between the diffusivities, D_δ, determined from the attenuation and the diffusivities, D_φ, determined

from the phase shift of the pressure signals since observations do not lie on the theoretical relation for radial flow.

For a specific borehole, D_δ-values systematically decrease with increasing period by about two orders of magnitude (Fig. 5a). When switching injection and monitoring between BK1 and BK3, diffusivities from attenuation systematically differ from each other while diffusivities from phase shift are almost indistinguishable (Fig. 5b). This difference is, however, small compared to the variation with period and may be related to the difference in well depth. At first glance, the large variability in D_δ-values with pumping period could be attributed to limits in the resolution of monitored pressure signals. However, the period dependence is also observed for pressure amplitudes well above the nominal resolution limit (Fig. 5c). Furthermore, we do not find a systematic effect of the amplitude of the oscillation in the injection well (Fig. 5d). Monitoring amplitudes may also be underestimated due to the finite storage capacity of the monitoring boreholes. Variation in storage capacity using hollow cylinders and pneumatic bladders with a through-going tube show that diffusivity is indeed increasingly underestimated for decreasing oscillation periods (Fig. 6). The underestimation, however, never reaches a factor of three, that is, half an order of magnitude, and thus, storage effects remain subordinate compared to the observed period dependence (Fig. 5a).

Injectivity (QP-)analysis

Pressure exhibits a characteristic delay with respect to flow rate in the pumping well because fluid is lost into and gained from the formation when pumping pressure is periodically increased and decreased, respectively. The full description of the corresponding injectivity can be realized using complex numbers, composed of modulus and phase. Amplitude ratios δ_{qp} between injection rate and pressure, the modulus of injectivity, decrease with increasing period from ~ 4 to ~ 0.2 l min^{-1}/bar with δ_{qp}-values of well BK1 systematically higher than that of BK3 (Table 1). From a comparison between the injectivity modulus and the geometric storage capacity,
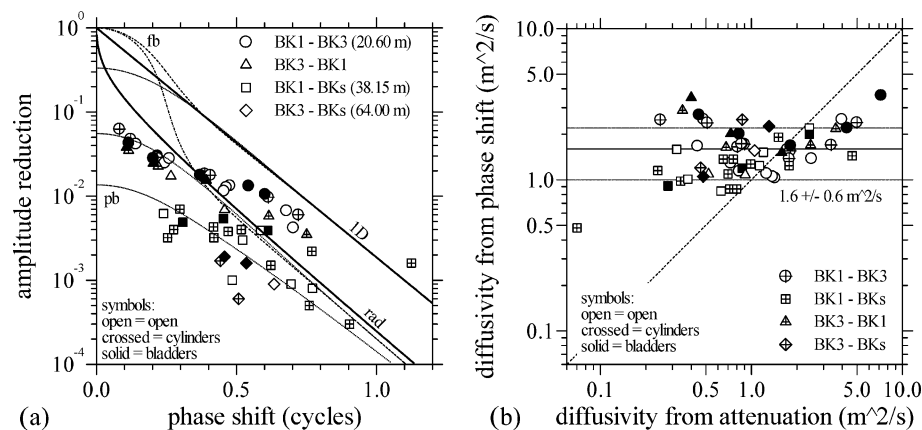

Figure 4. Results of pressure interference testing. (a) Observed relations between injection and monitoring pressure in comparison to radial (rad.) and 1-D flow in a homogeneous, isotropic subsurface (eqs 2, 3 and A8). The legends indicate the set-up of wells (see Fig. 1c) and distances between the pairs of wells (injection–monitoring) for which the comparison of the pressure records was performed. The line for the radial flow model weakly depends on the distance between pumping and monitoring well. Here, the solution for a distance of $\sim 300 \cdot r_i$ is given. The actual distances amount to ~ 410, ~ 760 and $1280 \cdot r_i$. The dotted and dashed curves give solutions for a constant pressure (pb) and a no-flow boundary (fb). All but the lowest curve for a pressure boundary ($R = 1100 \cdot r_i$) were calculated for a distance to the boundary of $R = 1500 \cdot r_i$ and a distance between wells of $1000 \cdot r_i$. The difference in the curves for the various radial models at high phase shifts documents the weak dependence of the solution on the distance between wells. (b) Comparison of hydraulic diffusivities determined from attenuation, D_δ, and phase shift, D_φ, of injection and monitoring pressure signals relying on the analytic solution for radial flow into a homogenous, isotropic subsurface (eqs 2 and 3). Diffusivity values from phase shift amount to 1.6 ± 0.6 m^2 s^{-1} and show considerably less variation than diffusivity values determined from attenuation.
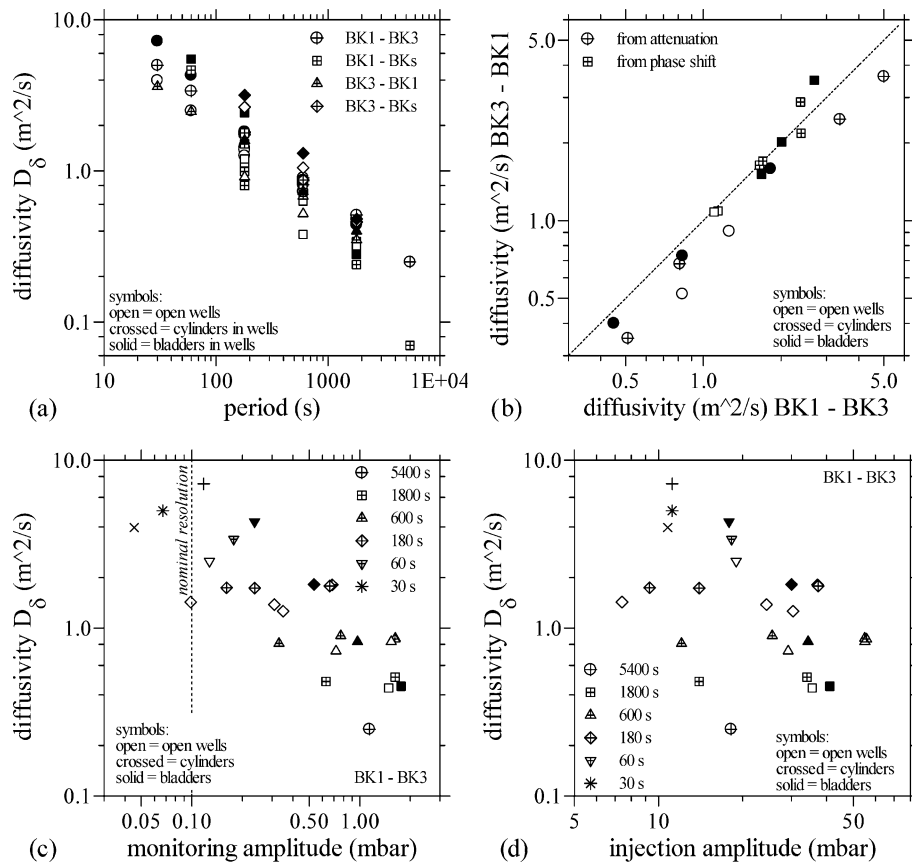
Figure 5. (a) Variation of the hydraulic diffusivity determined from attenuation of pressure signals with oscillation period. In the legends, the injection well is named first and the monitoring well second. (b) Comparison of results for tests in boreholes BK1 and BK3 switching injection and monitoring. Variation of the hydraulic diffusivity determined from attenuation of pressure signals with (c) monitoring and (d) injection amplitude. For the tests with a period of 30 s the '×' denotes 'open well', '∗' 'cylinders', and '+' 'bladder'.
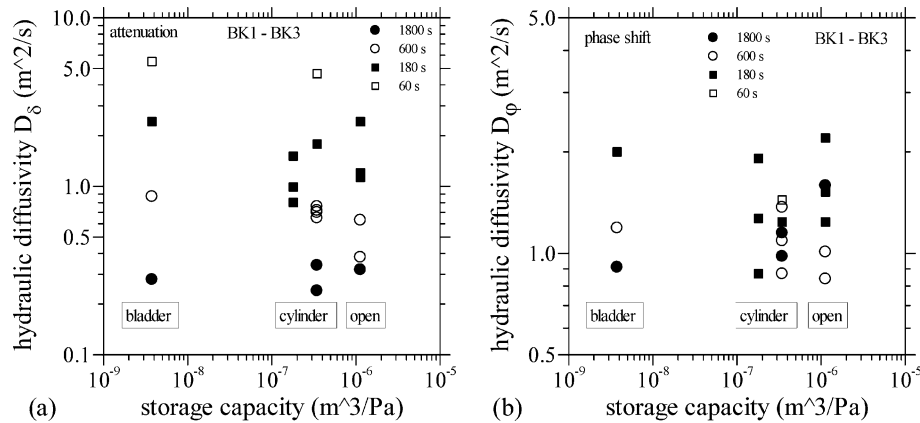
Figure 6. The dependence of hydraulic diffusivity determined from (a) attenuation and (b) phase shift of pressure records in the pumping and monitoring wells on the storage capacity of the monitoring wells (note the difference in *y*-axis scales). Storage capacity is here defined as the ratio between the change in fluid volume to the change in pressure in the well, $B_m = \Delta V / \Delta p = A_m / \rho g$. The effective cross section of the monitoring well, A_m, was varied by leaving the wells open, inserting hollow cylinders, or almost fully sealing the wells with inflatable bladders (see Fig. 1c).

$B_i = \frac{A_i}{\rho g} \simeq 8 \cdot 10^{-6}$ l/mbar, we find that the fluid volume injected and produced is on the order of or exceeds the fluid volume temporarily stored in the well during a period (Fig. 7a). Note, a tight well would be characterized by an injectivity of 0, and the compressive storage capacity corresponding to the compressibility β_w of water, $B_c = A_i h \beta_w \simeq 6 \cdot 10^{-10}$ l/mbar, is negligible. Upon accounting for the difference in the height of water columns of BK1 and BK3,

fair agreement between injectivity moduli of the two wells is found (Fig. 7a).

Phase shift φ_{qp} between injection rate and pressure, the argument of the injectivity, is as little as ~2 per cent of a cycle for the longest periods and approaches 20 per cent of a cycle for the shortest periods (Fig. 7b). At intermediate periods of 30–180 s, phase shift values for BK3 are lower than those for BK1. At a given period, phase shift
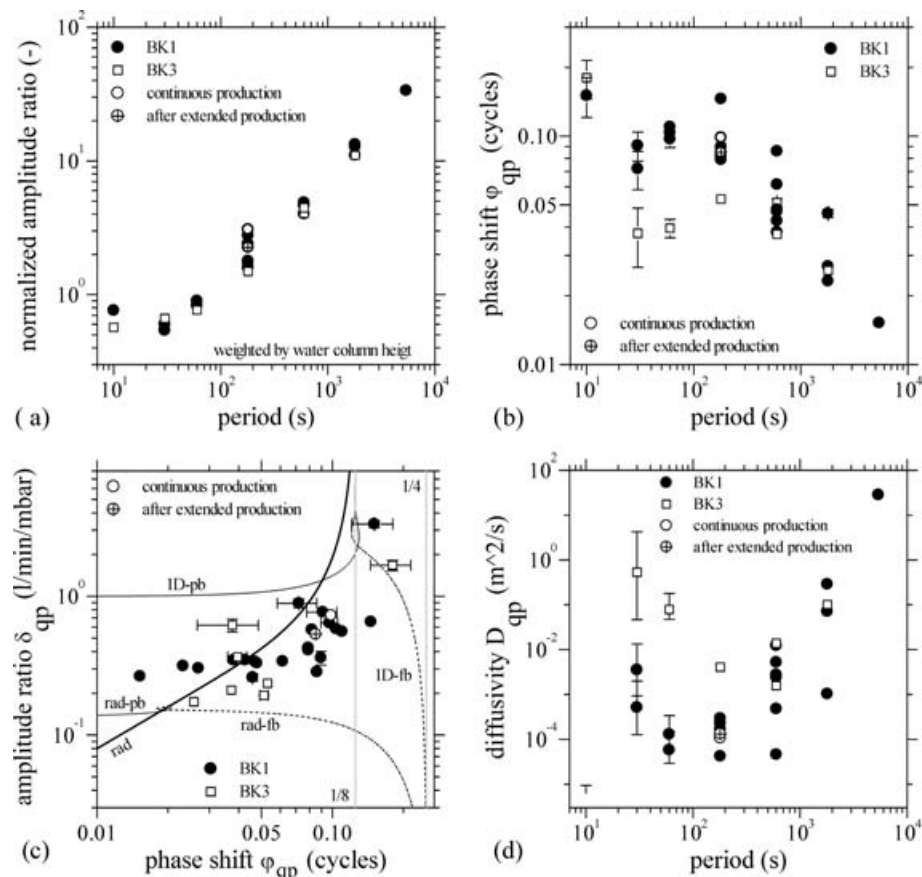
Figure 7. Results of injectivity (QP-)analysis. (a) Amplitude ratio δ_{qp} normalized by the geometric storage capacity of the pumping well and weighted by the height of the water column and (b) phase shift φ_{qp} as a function of pumping period. (c) Amplitude ratio δ_{qp} versus phase shift φ_{qp}. The thick line represents radial (rad) flow in a homogenous medium (eq. A3). Predictions for 1-D flow are labelled 1-D. The dotted and dashed curves give solutions for a constant pressure (pb) and a no-flow (fb) boundary at a distance of $R = 1500 \cdot r_i$, respectively (see eqs A2–A4). Changing the assumed hydraulic parameters shifts the theoretical curves vertical without distortion. (d) Equivalent hydraulic diffusivity D_{qp} calculated relying on eqs (4) and (5) as a function of pumping period.
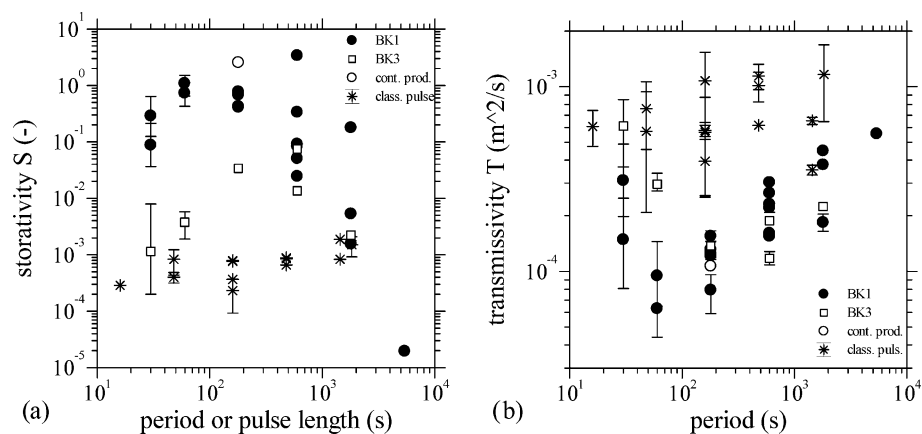
Figure 8. Equivalent storativity (a) and transmissivity (b) determined assuming radial flow in a homogeneous isotropic subsurface (eqs 4 and 5). Results of the classical pulse analysis (class. pulse) are shown for comparison.

values vary with injection amplitude. Although pairs of amplitude ratio and phase determined at various periods do not exhibit the relation predicted for radial flow in an isotropic, homogeneous material (Fig. 7c), an equivalent homogenous medium exists for every individual pair. The corresponding equivalent hydraulic diffusivity values range from $>10^{-4}$ to <10 m^{2}s^{-1} first decreasing and then increasing with increasing period (Fig. 7d). Diffusivity values are

lower for BK1 than for BK3 at short periods but roughly coincide for $T_0 > 100$ s. The period dependence of diffusivity is primarily caused by variations in storativity (Fig. 8a). Storativity values range between $>10^{-5}$ and ~ 1 with values for BK3 systematically lower than for BK1 by one to two orders of magnitude at periods of less than 600 s. Transmissivity values vary by less than one order of magnitude (Fig. 8b) amounting to 10^{-4} to 10^{-3} m^{2}s^{-1} with a

tendency to first decrease and then increase with period and without a systematic difference between BK1 and BK3.

Periodic pumping superposed on continuous production

The superposition of periodic variations in pumping rate on a continuous production intended to demonstrate the possibility to superpose a periodic variation on a transient change but also to address two questions:

(1) Does the interface between the land-filling and the top of the sandstone formation significantly affect the lateral water transport?

(2) Does the irregularity of callipers at the wells' tops significantly bias the QP-analysis?

Continuous production with ~20 l min^{-1} in BK1 reduced the water level below the interface where the well calliper is approximately constant. Then production rate was periodically varied between ~20 and 15 l min^{-1}. The evaluation of this test yields hydraulic parameters similar to those gained from tests at higher water levels (Fig. 7, Table 1) suggesting that the interface is not a preferential conduit and that effects related to irregular callipers are subordinate.

3.2 Conventional transient methods

In order to compare the results of the periodic pumping tests to conventional methods, we performed drawdown tests (Fig. 9) and analysed pressure records based on the theory for single pulse tests. The lowering of the water level in a monitoring well as a consequence of continuous production with constant flow rate in a borehole at distance *r* can be evaluated according to the 'Cooper-Jacob straight line time-drawdown method'(Fetter 2001). From a production test in BK1, we evaluated the initial linear relation observed over some hundred seconds in BK3. Using the flow measured at the surface, we calculate a transmissivity of $2.2 \cdot 10^{-3}$ m^{2}s^{-1} and a storativity of $9.2 \cdot 10^{-4}$ corresponding to a hydraulic diffusivity of 2.4 m^{2}s^{-1} in close agreement with results of the QP-analysis for periods larger
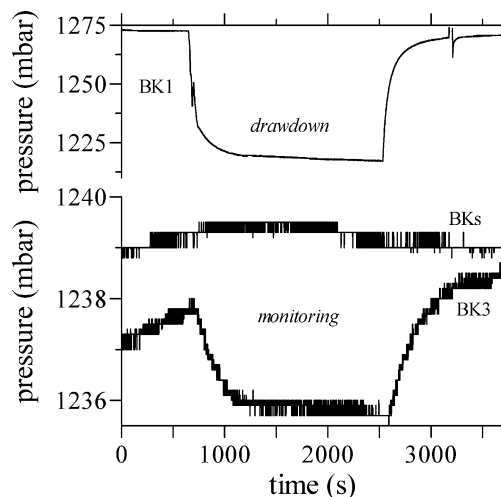

Figure 9. Example of a draw-dawn test in BK1. Note, the timescales of the periodic experiment in Fig. 2(b) and the drawdown experiment presented here are identical. In either of the two cases, the pressure variation in the most distant observation well, BKs, barely exceeds the digital resolution and are superposed by a transient increase from a preceding pumping operation. While the periodicity in the signal given in Fig. 2(b) is even visible with the bare, it is impossible to perform a reliable evaluation of the drawdown.

than 180 s (Fig. 7c) and with the average value from the phase shift analysis of the periodic interference testing (Fig. 4b).

In a number of cases, the first pumping operation of a periodic test could be used to perform a classical pulse interference analysis (Johnson *et al.* 1966; Stegemeier 1982) by evaluating (a) the time delay between termination of pumping and the occurrence of the maximum pressure in the monitoring well and (b) the ratio between the amplitudes of injection and monitoring pressure excursions. Determined values of hydraulic diffusivity (see Fig. 10a) decrease with increasing pulse length mainly because storativity increases (Fig. 8a); transmissivity is fairly constant at just below 10^{-3} m^{2}s^{-1} in good agreement with results of the injectivity analysis (Fig. 8b).

4 DISCUSSION

Periodic interference tests provide an immediate consistency check between observations and the considered models since their solution space is restricted to characteristic lines in the dimensionless attenuation-phase shift domain (Fig. 4a). The observations during the performed tests obviously do not comply with any of the considered models (Figs 4a and 7c), notably radial flow in a homogeneous medium, the standard model for the evaluation of conventional pumping tests. For further discussion, it is important to distinguish between geometrical aspects of our tests that violate the model assumptions on the one hand and complexity of the subsurface (e.g. heterogeneity) on the other hand. Therefore, we first summarize the geometrical characteristics of our tests but note already that a degeneration of the solution space from lines to areas does occur if distinct reservoirs, that is, zones with storativity deviating from average properties, are introduced in the model (Fischer 1992; Kranz *et al.* 1990).

The applied water level changes reach less than ~3 per cent of water column height, thus effects of horizontal flow in the vicinity of the changing water level can be neglected. The wells differ in depth/height of water column. Thus, monitoring the pumping in BK3 with the deeper well BK1 may involve some vertical flow component. However, the difference between observations when BK1 or BK3 are used as pumping well are small compared to variations with pumping period (Figs 5a and b). The comparatively small effect of reversing flow direction relative to the regional gradient in hydraulic head of less than 1 m over ~40 to 60 m also shows that gravity effects are subordinate. Obvious candidates for boundaries, the quarry wall and the reservoir, exhibit distances to the pumping wells that are at least as large as well depths and distances between the wells (Fig. 1a).

The distance between wells is on the order of or exceeds well depths, thus the sources are not of infinite extent. However, the penetration depth as estimated according to eq. (6) ranges from submetre scale to above well distance for the explored range in pumping periods (Fig. 10b). As a consequence, the vertical dimension of the source is much larger than the characteristic horizontal dimension of flow for periods up to 600 s, as required for an infinite source model. The notion that the interface between landfill and sandstone formation may constitute a vertical inhomogeneity is not supported by the pumping experiment with reduced water level which yield similar results compared to tests with a water level close to or above the interface (Fig. 7).

In conclusion, the geometrical aspects of our tests do not severely violate the assumptions of the standard radial flow model motivating a discussion of the results in terms of subsurface complexity (heterogeneity). For clarity, we consider boundaries of constant pressure
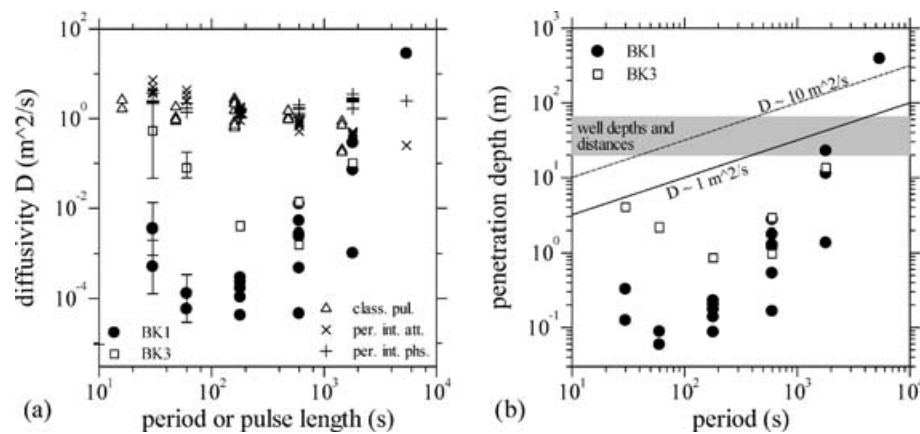
Figure 10. (a) Summary of diffusivity data determined from QP-analysis (labelled with the well number), classical pulse analysis (class. pul.), and periodic interference testing (per. int.) evaluating either attenuation (att.) or phase shift (phs.). (b) Penetration depth according to eq. (6) calculated using equivalent diffusivities D_{qp} determined from the QP-analysis of tests in BK1 and BK3. For comparison, lines represent the relations for a homogeneous subsurface with $D \sim 1$ or 10 m^{2}s^{-1}. The grey shaded area corresponds to the range of dimensions associated with the wells.

or flow, vertical constraints on the flow, and anisotropy as particular cases of heterogeneity. Alternative models involving a homogeneous medium may partly explain the observed period dependence but will probably not be capable of explaining the variation in modulus and phase of injectivity at a given period (Fig. 7). This amplitude dependence in QP-analysis may indicate non-linearity caused by heterogeneity or a pressure dependence of hydraulic properties or a breakdown of Darcy's law. We found little evidence for pressure dependence of hydraulic properties (Fig. 5c) and dealing with non-Darcian flow (e.g. Neuman & Zhang 1990) is clearly beyond the scope of our exploratory study. Therefore, we proceed by interpreting the differences between the results of the two periodic methods and the deviations from the predictions for a homogenous isotropic subsurface as indicating a heterogeneous subsurface.

4.1 Hydraulic characteristics of the jointed formation

In our investigation, the hydraulic transport is certainly dominated by the joints. The matrix porosity is too low to contribute significantly on the timescales of the tests. Conceptually, jointed formations may reach statistical homogeneity beyond a length scale of at least an order of magnitude larger than the characteristic joint spacing (e.g. Bear 1993; Bear & Berkowitz 1987). The penetration depth at the shortest periods is as small as the characteristic spacing of the joints, that is, dm-scale. At these small periods, interference observations approach the relation for a 1-D flow model (Fig. 4a) and the results of the injectivity analysis exhibit some agreement with a 1-D flow model too (Fig. 7c, particularly BK1). However, we can probably exclude truly 1-D flow, that is, a single tube-like conduit or a vertical planar conduit intersecting the injection well, because similar interference responses are measured in obtuse directions. Notably, for small frequencies the phase of injectivity exceeds 1/8, the limit for radial flow and unbounded 1-D flow in a homogeneous medium. Crosnier *et al.* (1985) predict a larger limit of 1/4 for flow on horizontal fractures (see also Hollaender *et al.* 2002; Jouanna 1993). Our observations may, therefore, partly map the scale-dependent transition in constitutive behaviour of a jointed formation. We refrain from a more detailed comparison with the model of Crosnier *et al.* (1985) since the derived analytic solution rests on the assumption of incompressible materials. As a consequence of this assumption, the pressure oscillation exhibits

attenuation in form of cylindrical divergence (logarithmic decay with increasing distance) but is instantaneous, that is, phase shift is zero everywhere in strong contradiction to our interference observations.

The stagnation of attenuation of pressure signals (Fig. 4a) and the approximately constant phase of injectivity (Fig. 7c) observed for large periods may suggest a constant pressure boundary. Also, the pressure in the pumping well seems to approach constant values for continued drawdown (Fig. 9b). The obvious candidate for a constant pressure boundary, the freshwater reservoir, has a distance to the wells of $R > 1500 \cdot r_i$ and breaks radial symmetry (see Fig. 1). Quantitative agreement between interference observations in BKs and predictions is reached considering a constant pressure boundary at a distance of $R = 1100 \cdot r_i$, that is, only ~10 per cent larger than the distance between pumping and monitoring wells (Fig. 4a). BKs is nearest to the quarry wall with a distance of less than ~10 m. Intuitively, the quarry wall that also breaks radial symmetry may, however, be considered as a no-flow boundary because of the abrupt change in overburden pressure. Introducing a no-flow boundary in the models leads consistently to even greater disagreement between model curves and observations (Figs 4a and 7c).

The effect of period variation on diffusivity is larger for injectivity tests than for interference tests (Fig. 10a). We suppose that during interference testing, the response in the monitoring well is dominated by the hydraulic properties of the subsurface volume along the tie line between the pumping and monitoring well. A variation of pumping period will thus investigate the 'intrinsic' period dependence in hydraulic properties of the subsurface volume between the wells. In contrast, during a periodic injectivity test the spatial extent of the subsurface volume that determines the flow signal depends on the pumping period. The considered penetration depth (eq. 6) constitutes an estimate of its horizontal extension. (Note, pressure can be well transmitted beyond the penetration depth. It is only a question of resolution of the gauge whether it is measurable. In contrast, flow rate measured at the pumping well is significantly affected only by the subsurface volume represented by penetration depth.) We cannot exclude that interference tests are contaminated by spatial heterogeneity offside the tie line between the pair of wells considered. The different estimates for hydraulic diffusivity agree at a period of about 1800 s corresponding to a penetration depth on the order of the interwell distances (Fig. 10). This agreement substantiates

the notion that interference tests examine the volume between the wells rather independent of period while injectivity tests reach successively larger volumes with increasing period.

Hydraulic diffusivities determined from attenuation observed in pressure interference tests systematically decrease with increasing period (Fig. 5a). A similar relation between the pulse length and hydraulic diffusivity is found for classical pulse tests (Fig. 10a) (Nakao *et al.* 2004). In the latter, the decrease in diffusivity with increasing pulse length is mainly caused by an increase in storativity (Fig. 8). A reasonable physical model may explain the systematic decrease in diffusivity with the characteristic timescale of pumping. Nearly constant transmissivity may be controlled by a 'backbone' of conduits insensitive to period variations. In contrast, the more time given for pressure equilibration the more conduits are used for storage that do not contribute to transport (compare Fatt 1959; Turner 1958).

In comparison to the storativity values determined from classical pulse analysis that we consider to represent an average for the subsurface volume between the considered pair of wells, storativity values determined from QP-analysis are considerably higher in particular for BK1 for periods up to 600 s (Fig. 8). These high storage capacity values keep the diffusivity and consequently the penetration depth small at low periods (Figs 7c and 10b). Increased storativity in the vicinity of the wells may have resulted from drilling.

The determined equivalent hydraulic properties are apparent in the sense that if the subsurface were homogeneous it had these properties. Our observation of a combination of almost constant transmissivity with strongly varying storativity may correspond to observations in numerical modelling of drawdown tests where the implemented heterogeneity in transmissivity is reflected by an apparent variability in storativity (e.g. Meier *et al.* 1998; Sánchez-Vila *et al.* 1999b). It seems necessary to extend the concept of storativity for heterogeneous media. By definition, storativity is a static property while any pumping operation will be associated with a characteristic timescale. Variations in transmissivity will always cause an apparent variation in storativity for transient pressure changes because the two processes of transport and storage are linked. Fluid can only be stored in subsurface volumes that are reached by transport on the timescale of the pumping operation.

4.2 Feasibility and applications of periodic pumping tests

Periodic pumping can be performed with the field equipment used for standard procedures. The periodic excitation can be easily realized by manual control of the pump according to a prescribed schedule. In principle, a monochromatic signal is not mandatory but any periodic excitation can be evaluated. Our results show that the periodic pumping approach yields results that are comparable to those of the conventional methods when relying on the same model for the analysis of hydraulic parameters and timescales of pumping operations are comparable (Figs 8 and 10a). Injectivity testing constitutes a unique tool for scanning the subsurface to an increasing penetration depth. From periodic interference tests, a small response can be constrained in shorter time than for classical pulse testing and without requiring an equilibrated system because signal analysis procedures can be employed (Figs 2b and 9). Furthermore, the periodic interference analysis does not require quantification of flow rates. Periodic interference testing suffers an apparent loss of information compared to classic pulse testing because only the hydraulic

diffusivity can be determined instead of transmissivity and storativity separately. However, the solution spaces of the considered simple analytical models are constituted by curves representing all pairs of phase shift and attenuation consistent with the underlying model. The comparison with the theoretical curves thus provides unique information to what extent a model is applicable. In principle, the information on model consistency can be gained from a single periodic test but tests at different periods should be considered to exclude coincidental agreement. The straightforward evaluation of model applicability based on a limited number of pumping tests is a strong methodical gain in comparison to pulse or drawdown tests. In classical pulse testing such a consistency check is usually not possible because it had to rely on a detailed analysis of the temporal evolution of the response. Often, already determination of the first order characteristics of a pressure response (reference pressure and time of maximum pressure) is highly uncertain (see e.g. Fig. 9b). In drawdown testing, the late time behaviour with the logarithm in time is diagnostic for model consistency. However, interpretation of a linear relation on log scale involves some ambiguity. Furthermore, the problem is encountered that with increasing pumping duration the affected subsurface volume increases and with it the appropriate model may change.

On the practical side, periodic pumping tests exhibit several characteristics that set them apart from conventional tests. Firstly, the maximum pressure perturbation in the subsurface is determined by the imposed amplitude in contrast to being the *a priori* unknown outcome of a pumping operation. Thus, pressure limitations imposed by well design can be met and effects related to the pressure dependence of hydraulic properties can be avoided or alternatively studied on purpose. In addition, small periodic perturbations can be superposed on a continuous pumping operation limiting the disturbance of long-term operations. Secondly, the duration of a periodic pumping operation is known beforehand in contrast for example to the duration of drawdown or shut-in tests facilitating planning of a campaign. Analysis of transient pumping often depends on evaluating the relation between observables and the logarithm of time; improving data quality thus requires extending the duration by factors of 10 while the robustness of the Fourier analysis increases initially with every full period. Lastly, the amount of fluid at the surface can be limited if during a period amounts of produced and injected fluid balance as in our tests.

From the discussed characteristics, some obvious applications arise for periodic pumping tests. The employed technique of zero net flow over a period is advantageous when contaminated fluids are involved. The superposition of periodic variations can be used in fields with multiple active wells where ongoing pumping operations cause transients that hamper conventional analyses. Furthermore, continuous monitoring of the evolution of hydraulic properties is possible in production or injection fields either actively by superposing a small periodic perturbation on the pumping operation or passively in situations of cyclic operation (e.g. Orzol *et al.* 2004).

From a fundamental research perspective, testing at a range of periods contributes to the understanding of the 'intrinsic' period dependence of hydraulic properties. An improved understanding of dynamic hydraulic properties is important for the evaluation of the differences in the response of the subsurface to natural 'periodic' signals with largely different timescales, such as elastic waves, tides, barometric pressure, and seasonal charging/discharging by precipitation and evaporation (Brodsky *et al.* 2003; Roeloffs 1998; Rojstaczer & Agnew 1989; Schulze *et al.* 2000).

5 CONCLUSIONS

We conducted periodic pumping tests in a field of three shallow wells penetrating jointed sediments and presented the theoretical background for two evaluation methods of these tests, injectivity and interference analysis. These methods rely on a characterization of the relation between flow rate and pressure in a periodically pumped well and the relation between pressures in a periodically pumped well and a monitoring well, respectively. Amplitude ratio and phase shift between the considered signals permit a direct consistency check with considered models for the subsurface and constrain equivalent hydraulic properties. When relying on a model for radial flow in a homogeneous medium, the interference analysis constrains hydraulic diffusivity while the injectivity analysis yields estimates of transmissivity and storativity. The periodic interference analysis does not require flow measurements. The two test types provide information on the hydraulic properties of spatially distinct volumes. Periodic injectivity testing averages over a volume surrounding the pumping well with a size depending on the period of oscillation, thereby constituting a tool for scanning the subsurface to a penetration depth increasing with increasing period. In contrast, periodic interference testing averages over the vicinity of the tie-line between the pumping and a monitoring well. Thus, pressure-interference tests at various periods constrain the 'intrinsic' period dependence of the hydraulic properties of a particular volume while the period dependence of results from injectivity testing is controlled by the spatial variability of hydraulic properties.

By taking advantage of signal analysis procedures, periodic interference testing does not require an equilibrated system as do conventional methods and thus smaller responses can be separated from a 'noisy' record. Periodic pumping tests exhibit several operational advantages compared to conventional tests with respect to the maximum pressure occurring during a test, the known duration, and the zero net flow of a test. In addition, periodic pumping can be superposed on long-term operations permitting continuous monitoring of subsurface properties.

The results of our field tests show that the periodic pumping approach and conventional methods, such as drawdown and pulse testing, yield comparable results when relying on the same model for the analysis of hydraulic parameters. The injectivity testing suggests that the tested jointed sandstone formation is spatially heterogeneous. Data span more than five orders of magnitude in equivalent diffusivity for the close to four orders of magnitude variation in period. Equivalent transmissivity values vary by less than one order of magnitude. Thus, the storativity factor seems to be responsible for the period dependence of the hydraulic diffusivity. High storativity in the vicinity of the wells may be a result of the drilling. In interference tests, the variation of diffusivity with pumping period is weaker but diffusivity still decreases by two orders of magnitude over an increase in period of four orders. We suggest a conductive 'backbone' and increasing storage in dead-ends with increasing period as an explanation. Our observations may be related to the transition in constitutive behaviour of jointed media controlled by spatial scale. Numerical modelling of heterogeneous media will be educative for an improved interpretation of periodic pumping tests. It seems particularly crucial to distinguish between the static storativity and the result of a pumping test associated with a specific timescale.

REFERENCES

Abramowitz, M. & Stegun, I.A., 1965. *Handbook of Mathematical Functions,* National Bureau of Standards, Dover Publications, Minealy, NY.

Barker, J.A. & Black, J., 1983. Slug tests in fissured aquifers, *Water Resourc. Res.,* **19**(6), 1558–1564.

Bear, J., 1993. Modeling flow and contaminant transport in fractured rocks, in *Flow and Contaminant Transport in Fractured Rock*, pp. 1–37, eds Bear, J., Tsang, C.-F. & de Marsily, G., Academic Press, San Diego.

Bear, J. & Berkowitz, B., 1987. Groundwater flow and pollution in fractured rock aquifers, in *Developments in Hydraulic Engineering*, pp. 175–238, ed. Novak, P., Elsevier Applied Science, Amsterdam.

Bernabe, Y., 1997. The frequency dependence of harmonic fluid flow through networks of cracks and pores, *Pure appl. Geophys.,* **149**, 489–506.

Bredehoeft, J.D., Cooper, H.H. & Papadopulos, I.S., 1966. Inertial and storage effects in well-aquifer systems: an analog investigation, *Water Resourc. Res.,* **2**(4), 697–707.

Brodsky, E.E., Roeloffs, E., Woodcock, D., Gall, I. & Manga, M., 2003. A mechanism for sustained groundwater pressure changes induced by distant earthquakes, *J. geophys. Res.,* **108**(B8), doi:10.1029/2002JB002321.

Buttkus, B., 2000. *Spectral Analysis and Filter Theory in Applied Geophysics*, 667 pp., Springer, Berlin.

Carslaw, H.S. & Jaeger, J.C., 1959. *Conduction of Heat in Solids*, 510 pp., Clarendon Press, Oxford.

Copty, N.K. & Findikakis, A.N., 2004. Stochastic analysis of pumping test drawdown data in heterogeneous geologic formations, *J. Hydraul. Res.,* **42,** 59–67.

Crosnier, B., Fras, G. & Jouanna, P., 1985. Reconnaissance of fractured media with several systems of fractures by means of harmonic techniques, *Rock Mech. Rock Eng.,* **18,** 77–105.

Dagan, G., 1986. Statistical theory of groundwater flow and transport: pore to laboratory, laboratory to formation, and formation to regional scale, *Water Resourc. Res.,* **22**(9), 120S–134S.

Fatt, I., 1959. A demonstration of the effect of 'dead-end' volume on pressure transients in porous media, *J. Petrol. Tech.* ((Dec.)), 66–70.

Fetter, C.W., 2001. *Applied Hydrogeology*, 598 pp., Prentice Hall, Upper Saddle River, New Jersey.

Fischer, G.J., 1992. The determination of permeability and storage capacity: Pore pressure oscillation method., in *Fault Mechanics and Transport Properties of Rocks.*, pp. 187–211, eds Evans, B. & Wong, T.-F., Academic Press, San Diego.

Gelhar, L.W., 1986. Stochastic subsurface hydrology from theory to applications, *Water Resourc. Res.,* **22**(9), 135S–145S.

Hilfer, R., 1996. Transport and relaxation phenomena in porous media, in *Advances in Chemical Physics*, pp. 299–424, eds Prigogine, I. & Rice, S. A., Wiley, New York.

Hollaender, F., Hammond, P. & Gringarten, A.C., 2002. Harmonic testing for continuous well and reservoir monitoring, *SPE, 77692*.

Horne, R.N., 1992. *Modern Well Test Analysis*, Petroway Inc., Palo Alto.

Isakoff, S.E., 1955. Analysis of unsteady fluid flow using direct electrical analogs, *Industr. Engng. Chem.,* **47**(3), 413–421.

Johnson, C.R., Greenkorn, R.A. & Woods, E.G., 1966. Pulse-testing: a new method for describing reservoir flow properties between wells, *J. Petrol. Tech.* (Dec.), 1599–1604.

Jouanna, P., 1993. A summary of field test methods in fractured rocks, in *Flow and Contaminant Transport in Fractured Rock*, pp. 437–541, eds Bear, J., Tsang, C.-F. & de Marsily, G., Academic Press, San Diego.

Kamal, M. & Brigham, W.E., 1975. Pulse testing response for unequal pulse and shut-in periods, *Soc. Petrol. Eng. J.* (Oct), 399–410.

Kranz, R.L., Saltzman, J.S. & Blacic, J.D., 1990. Hydraulic diffusivity measurements on laboratory rock samples using an oscillating pore pressure method, *Int. J. Rock Mech. Min. Sci and Geomech. Abstr.,* **27**(5), 345–352.

Krauss-Kalweit, I., 1987. Bestimmung der Durchlässigkeit im Untergrund und im Stauwerk von Talsperren mit dem Einschwingverfahren, *Wasserwirtschaft,* **77,** 338–341.

Kuo, C.H., 1972. Determination of reservoir properties from sinusoidal and multirate flow tests in one or more wells, *Soc. Petrol. Eng. J.,* **12,** 499–506.

Macdonald, J.R., 1987. *Impedance Spectroscopy*, Wiley, New York, p. 346.

Matthews, C.S. & Russell, D.G., 1967. *Pressure Buildup and Flow Tests in Wells*, 173 pp., Soc. Petrol. Eng. AIME, New York.

Meier, P.M., Carrera, J. & Sánchez-Vila, X., 1998. An evaluation of Jacob's method for the interpretation of pumping tests in heterogeneous formations, *Water Resourc. Res.,* **34**(5), 1011–1025.

Nakao, S., Ishido, T. & Takahashi, Y., 2004. Pulse testing analysis for fractured geothermal reservoir—a case study at the Uenotai geothermal field, Japan, in *Dynamics of fluids in fractured rocks - Addendum*, pp. A-14–A-16, eds Faybishenko, B. & Witherspoon, P.A., Berkeley Lab, Berkeley, California.

Neuman, S.P., 1990. Universal scaling of hydraulic conductivities and disperivities in geologic media, *Water Resourc. Res.,* **26** (8), 1749–1758.

Neuman, S.P. & Zhang, Y.-k., 1990. A quasilinear theory of non-Fickian and Fickian subsurface dispersion, 1. Theoretical analysis with application to isotropic media, *Water Resourc. Res.,* **26**(5), 887–902.

Neuman, S.P., Guadagnini, A. & Riva, M., 2004. Type-curve estimation of statistical heterogeneity, *Water Resourc. Res.,* **40,** W04201, doi:10.1029/2003WR002405.

Oliver, D.S., 1993. The influence of nonuniform transmissivity and storativity on drawdown, *Water Resourc. Res.,* **29**(1), 169–178.

Olny, X. & Boutin, C., 2003. Acoustic wave propagation in double porosity media, *J. acoust. Soc. Am.,* **114**(1), 73–89.

Orzol, J., Jatho, R., Jung, R., Kehrer, P. & Tischner, T., 2004. The GeneSys Project - Development of concepts for the extraction of heat from tight sedimentary rocks, *Z. angew. Geol.,* **2,** 17–23.

Renard, P. & de Marsily, G., 1997. Calculating equivalent permeability: a review, *Adv. Wat. Resourc.,* **20**(5–6), 253–278.

Roeloffs, E.A., 1998. Persistent water level changes in a well near Parkfield, California, due to local and distant earthquakes, *J. geophys. Res.,* **103,** 869–889.

Rojstaczer, S. & Agnew, D.C., 1989. The influence of formation material properties on the response of water levels in wells to Earth tides and atmospheric loading, *J. geophys. Res.,* **94,** 12 403–12 411.

Sánchez-Vila, X., Axness, C.L. & Carrera, J., 1999a. Upscalig transmissivity under radially convergent flow in heterogeneous media, *Water Resourc. Res.,* **104**(3), 613–621.

Sánchez-Vila, X., Meier, P.M. & Carrera, J., 1999b. Pumping tests in heterogenous aquifers: an analytical study of what can be obtained from their interpretation using Jacob's method, *Water Resourc. Res.,* **35**(4), 943–952.

Schad, H. & Teutsch, G., 1994. Effects of the investigation scale on pumping test results in heterogeneous porous aquifers, *J. Hydrol.,* **159,** 61–77.

Schulze, K.C., Kümpel, H.-J. & Huenges, E., 2000. In-situ petrohydraulic parameters from tidal and barometric analysis of fluid level variations in deep wells; some results from KTB, in *Hydrogeology of Crystalline Rocks*, pp. 79–104, eds Stober, I. & Bucher, K., Kluwer, Dordrecht.

Stegemeier, G.L., 1982. *Interwell pressure testing for field pilots*, SPE, 11086.

Stewart, C.R., Lubinski, A. & Blenkarn, K.A., 1961. The use of alternating flow to characterize porous media having storage pores, *Trans. AIME,* **222,** 383–389.

Turcotte, D.L. & Schubert, G., 1982. *Geodynamics*, 450 pp., Wiley, New York.

Turner, G.A., 1958. The flow-structure in packed beds, *Chem. Engng. Sci.,* **7,** 156–165.

Ye, M., Neuman, S.P., Guadagnini, A. & Tartakovsky, D.M., 2004. Nonlocal and localized analyses of conditional mean transient flow in bounded, randomly heterogeneous media, *Water Resourc. Res.,* **40,** W05104, doi:10.1029/2003WR002099.

APPENDIX

Radial flow

We choose a cylindrical coordinate system such that the z-axis coincides with the symmetry axis of an infinitely long injection borehole with radius r_i, that is, effects of vertical pressure gradients are ignored. Then, the diffusion equation for radial symmetry reads as

$$D^{-1}\frac{\partial p}{\partial t} = \frac{\partial^2 p}{\partial r^2} + \frac{1}{r}\frac{\partial p}{\partial r}. \tag{A1}$$

Steady-state solutions for sinusoidal pressurization with $p_{i(t)} = p_0 \exp(i\omega t)$ and a constant pressure boundary (pb) at $r = R$

$$p_{\mathrm{pb}(r,t)} = p_{i(t)} \frac{I_{0(\eta R)}K_{0(\eta r)} - I_{0(\eta r)}K_{0(\eta R)}}{I_{0(\eta R)}K_{0(\eta r_i)} - I_{0(\eta r_i)}K_{0(\eta R)}}, \tag{A2}$$

or a no-flow boundary (fb) at $r = R$

$$p_{\mathrm{fb}(r,t)} = p_{i(t)} \frac{K_{1(\eta R)}I_{0(\eta r)} + K_{0(\eta r)}I_{1(\eta R)}}{K_{1(\eta R)}I_{0(\eta r_i)} + K_{0(\eta r_i)}I_{1(\eta R)}}, \tag{A3}$$

can be derived by separation of variables where I_0, I_1 and K_0, K_1 denote modified Bessel functions of the first and second kind of zero and first order, respectively. The complex argument of the Bessel functions carries the characteristics of the experimental procedure and the subsurface, $\eta = \sqrt{i\omega D^{-1}}$. In the limit $R \to \infty$, only the Bessel functions of the second kind characterize the decrease in amplitude with increasing distance and attenuation and phase shift calculate as $\delta_{\mathrm{pp}} = |p_{(r,t)}|/|p_{(r_i,t)}| = |K_{0(\eta r)}/K_{0(\eta r_i)}|$ and $\varphi_{\mathrm{pp}} = \arg (K_{0(\eta r)}/K_{0(\eta r_i)})$ (Fig. 11), respectively (compare Carslaw & Jaeger 1959). Using Darcy's law we can calculate the flow rate as

$$Q_{(r,t)} = Aq_{(r,t)} = -A\frac{T}{h\rho g}\frac{\partial p_{(r,t)}}{\partial r}$$

$$\Rightarrow Q_{\mathrm{pb}(r,t)} = 2\pi r_i \frac{T}{\rho g}\eta \frac{I_{0(\eta R)}K_{1(\eta r)} + I_{1(\eta r)}K_{0(\eta R)}}{I_{0(\eta R)}K_{0(\eta r_i)} - I_{0(\eta r_i)}K_{0(\eta R)}} p_{i(t)} \text{ and}$$

$$Q_{\mathrm{fb}(r,t)} = 2\pi r_i \frac{T}{\rho g}\eta \frac{I_{1(\eta R)}K_{1(\eta r)} - I_{1(\eta r)}K_{1(\eta R)}}{K_{1(\eta R)}I_{0(\eta r_i)} + K_{0(\eta r_i)}I_{1(\eta R)}} p_{i(t)} \tag{A4}$$

where $A = 2\pi r_i h$ denotes the area of the borehole through which fluid is injected and we used $\partial I_{0(\eta r)}/\partial r = \eta I_{1(\eta r)}$ and $\partial K_{0(\eta r)}/\partial r = -\eta K_{1(\eta r)}$. In the limit $R \to \infty$, injection rate and injection pressure are related according to

$$Q_{i(t)} = 2\pi r_i \frac{T}{\rho g}\frac{\eta K_{1(\eta r_i)}}{K_{0(\eta r_i)}} p_{i(t)}, \tag{A5}$$

with a phase shift and an amplitude ratio of $\varphi_{\mathrm{qp}} = \arg(\eta K_{1(\eta r_i)}/K_{0(\eta r_i)})$ and $\delta_{\mathrm{qp}} = 2\pi r_i \frac{T}{\rho g}|\eta K_{1(\eta r_i)}/K_{0(\eta r_i)}|$, respectively. The calculation of hydraulic properties based on eqs (A2) and (A5) is illustrated in Fig. 12.

1-D flow

The 1-D diffusion equation for flow from a source at $x = 0$ along the x-axis reads as

$$\frac{\partial p}{\partial t} = D\frac{\partial^2 p}{\partial x^2}. \tag{A6}$$

For periodic flow from the surface of a half-space, the steady state solution reads (e.g. Carslaw & Jaeger 1959)
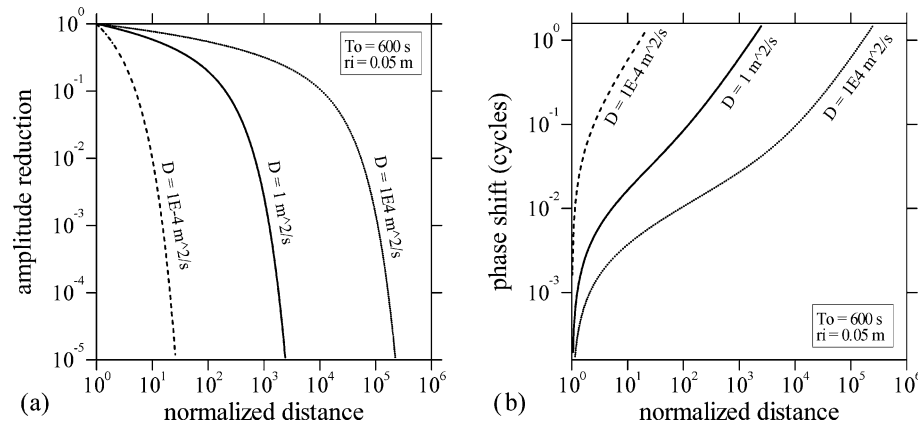
Figure 11. (a) Amplitude reduction (attenuation) and (b) phase shift between injection and monitoring pressure as a function of normalized distance, r/r_i, for a sinusoidal injection pressure with period $T_0 = 600$ s in pumping well with radius $r_i = 0.05$ m. In many applications, an amplitude reduction of 10^{-5} will roughly correspond to the resolution limit of the pressure transducer in the monitoring well. The reduction in amplitude accelerates at a characteristic distance, the penetration depth estimated according to eq. (6). Note, the given lines are valid for any pair of period and hydraulic diffusivity that yields the same product, DT_0, as the explicitly displayed parameters.
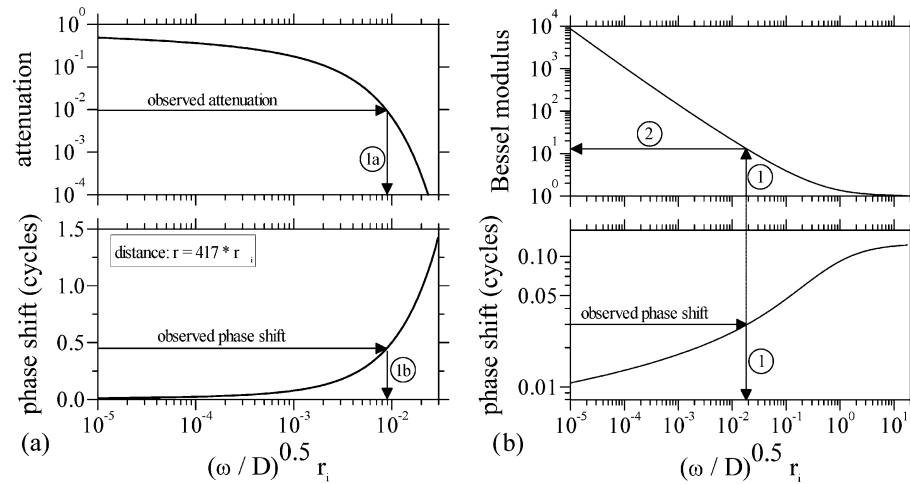

Figure 12. Graphical illustration of the numerical determination of hydraulic parameters from periodic pumping tests for assumed radial flow in a homogenous medium. (a) Interference (PP-) analysis: For a given distance between pumping and monitoring well, attenuation and phase shift can be calculated as a function of the parameter $\sqrt{\omega/D} \cdot r_i$ according to eqs (2) and (3), respectively. Observed attenuation and phase shift values can then be used to find corresponding hydraulic diffusivities D_δ and D_ϖ (arrow 1a and 1b). (b) Injectivity (QP-)analysis: The phase and modulus of the complex term $i^{0.5} K_{1(\eta r_i)}/K_{0(\eta r_i)}$ are numerically determined for a range of $\eta r_i = \sqrt{i\omega/D} \cdot r_i$ values. According to eq. (4) the observed phase shift between flow rate and pressure uniquely determines hydraulic diffusivity D (arrow 1), which is used to derive the modulus of $i^{0.5} K_{1(\eta r_i)}/K_{0(\eta r_i)}$, too (arrow 2). Transmissivity is calculated using the derived modulus in eq. (5); storativity finally calculates from $S = T/D$.

$$p_{(x,t)} = p_0 \exp\left(-x\sqrt{\frac{\omega}{2D}}\right) \exp\left[i\left(\omega t - x\sqrt{\frac{\omega}{2D}}\right)\right], \quad \text{(A7)}$$

yielding an amplitude reduction and phase shift at point x of

$$\delta_{pp} = \left|\frac{p_{(x,t)}}{p_{i(t)}}\right| = \exp\left[-x\sqrt{\frac{\omega}{2D}}\right] \text{ and}$$

$$\varphi_{pp} = \arg\left(\frac{p_{(x,t)}}{p_{i(t)}}\right) = x\sqrt{\frac{\omega}{2D}}, \quad \text{(A8)}$$

respectively. Solutions for a constant pressure or a no-flow boundary at the finite distance L are explicitly given, for example, by (e.g. Fischer 1992). Using Darcy's law, the flow rate calculates as

$$Q_{(x,t)} = -A\frac{T}{h\rho g}\frac{\partial p_{(x,t)}}{\partial x}$$

$$= A\frac{T}{h\rho g}\sqrt{\frac{\omega}{2D}}(1+i)\exp\left[-(1+i)x\sqrt{\frac{\omega}{2D}}\right] p_0 \exp(i\omega t), \quad \text{(A9)}$$

yielding an amplitude ratio and a phase shift of injection rate with respect to injection pressure of

$$\delta_{qp} = \left|\frac{Q_{(0,t)}}{p_{(0,t)}}\right| = A\frac{T}{h\rho g}\sqrt{\frac{\omega}{D}} \quad \text{and} \quad \varphi_{qp} = \arg\left(\frac{Q_{(0,t)}}{p_{(0,t)}}\right) = \frac{\pi}{4}, \quad \text{(A10)}$$

respectively.